CHAPTER - V

CHAPTER-V

EFFECT OF Ag DOPING ON THE STRUCTURE AND SUPERCONDUCTIVITY OF $YBa_2Cu_3O_{7-y}$

V. 1. Introduction

The study reported in the present chapter establishes the sintering conditions under which Ag can be doped in the grains instead of precipitating at the grain boundaries. The study then probes into the effect of Ag doping on superconductivity and structural parameters in a series of samples of $YBa_2Cu_{3-x}Ag_xO_{7-y}$, with Ag concentration in the range 0 to 0.12 atoms per unit cell. Crystallochemical analysis of the oxygen content and carrier concentration dependence on Ag doping is made to understand the observed changes.

V.2. Experimental

Samples of $YBa_2Cu_{3-x}Ag_xO_{7-y}$, $0 \leq x \leq 0.12$ were prepared from stoichiometric proportion of Y_2O_3, $BaCO_3$, CuO and Ag_2O powders through the ceramic route discussed in Chapter III. Some samples of $YBa_2Cu_3O_{7-y}$ (YBCO) and Ag-doped YBCO with x = 0.12 were quenched from high temperatures (300, 500, 700, 900 C) on a copper block for studying the effect of Ag on oxygen disorder in the CuO chains. After quenching, the samples were immediately mounted for AC susceptibility measurement. X-ray diffraction (XRD) data were collected at room temperature using Cu-K_α radiation (λ=1.5406 A) at Saha Institute of Nuclear Physics, Calcutta. The oxygen content in the samples were determined by iodometric titration

method. The details of the AC susceptibility and oxygen content measurements are discussed in Chapter III.

V. 3. Results and Discussion

V.3.1. Disposition of Ag in the grains and grain boundaries of YBCO

Unlike many other additives, Ag incorporation in YBCO can either occur through lattice site substitution in the grains or at grain boundaries. Even metallic clusters of Ag filling the voids in the granular YBCO system has been reported [1]. The confinement of Ag at the grain boundaries or in clusters occurs mostly in YBCO/Ag composites which influences the superconducting and normal state properties of the composites to a great extent (Chapter VI,VII). Many authors [2,3] have reported that in composites, a certain amount of Ag diffuse into the YBCO grains. In samples where Ag is added stoichiometrically for $YBa_2Cu_{3-x}Ag_xO_{7-y}$ phase formation, Gangopadhyay and Mason [4] and Joo et al. [5] have shown that Ag content within the grains is lower than the nominal value, a fraction of Ag precipitating at the grain boundaries. Ag precipitation at the grain boundaries in Ag doped YBCO has also been seen by Houng et al. [6] and Orlova et al. [7]. Wave length dispersive x-ray spectroscopic analysis shows that the intragranular concentration of silver increases linearly with increasing nominal concentration, but reaches a saturation level after the nominal concentration is above 2.5% [3]. Energy dispersive x-ray spectroscopy also revealed that some Ag particles go to the grains of YBCO [3]. All these observations suggest that Ag goes to the grains upto a certain limit.

XRD spectra of such samples are expected to contain features like change in the unit cell parameters brought about by Ag doping at the crystallographic sites in the grains and additional lines due to Ag occupying grain boundaries or occurring as clusters. The XRD data obtained for $x = 0.12$ in our samples did not show extra peaks for Ag (Fig. V.1). This of course does not rule out the occurrence of Ag clusters, if very small

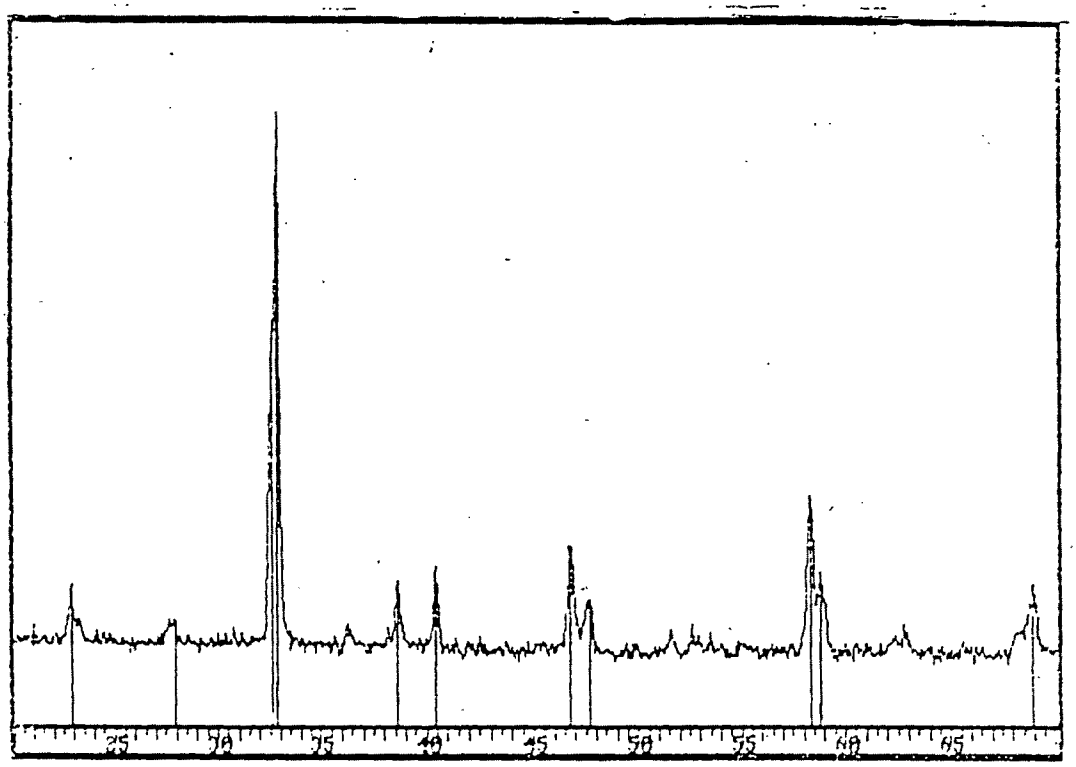

Fig. V.1. XRD spectrum of $YBa_2Cu_{3-x}Ag_xO_{7-y}$ with x = 0.12

amount of Ag precipitate at the grain boundaries. However, the increase of the volume of the unit cell with Ag doping (Table V.I) clearly indicates that Ag goes to the lattice sites in the grains.

Table V.I. Variation of oxygen content, upper (Tc_1) and lower (Tc_2) drop off in χ', and lattice parameters with Ag doping (x) in $YBa_2Cu_{3-x}Ag_xO_{7-y}$.

Ag content (x)	Oxygen content	Tc_1 (K)	Tc_2 (K)	Lattice parameter a (A)	b (A)	c/3 (A)	Unit cell Volume (A^3)
0	6.93	90	78	3.8210	3.8880	3.8900	173.37
0.06	6.91	85	68	3.8261	3.8865	3.8897	173.52
0.12	6.77	70	50	3.8308	3.8933	3.890	174.05

Temperature variation of both the real and imaginary components of the diamagnetic susceptibility signal (Fig. V.2) is seen to be highly dependent on Ag concentration. The χ' vs T for each of the sample has a distinct two stage drop off: the first stage starting from Tc_1 is followed by the second drop off beginning at a lower temperature Tc_2. This second stage results from the diamagnetic shielding produced by the intergrain supercurrent passing throughout the percolative network of weak links [8]. This stage is also marked with the peak in χ'' which is related to the hysteresis loss arising due to the penetration of magnetic flux in the intergranular network. The first drop off at the Tc_1 reflects the intragranular superconductivity. If most of the Ag precipitate at the grain boundaries, the interior of the grains will not be doped by Ag and hence the first drop off would coincide for all the Ag doped

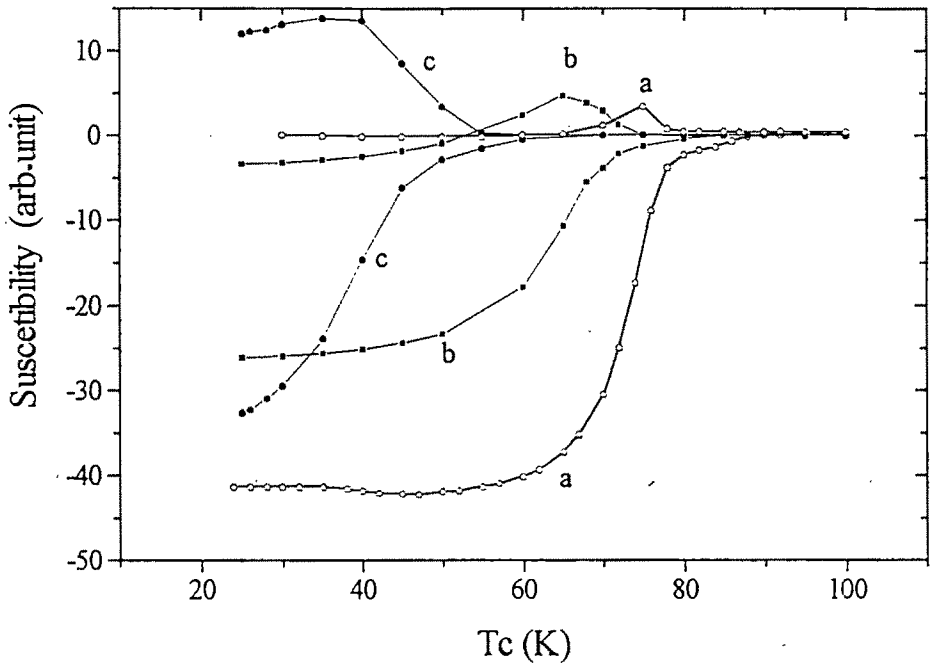

Fig.V.2. AC magnetic susceptibility variation with temperature in $YBa_2Cu_{3-x}Ag_xO_{7-y}$ samples. (a) x = 0, y = .072, (b) x = 0.06, y = 0.092, (c) x = 0.12, y = 0.230.

samples. The precipitated Ag at the grain boundaries would only affect the second drop off of χ' and the position of χ''. Fig. V.2 however shows that both the first and second drop off of χ' and the peak position of χ'' strongly depends on Ag doping, indicating the substitution of Ag at the lattice sites in the grains.

V.3.2. Possibilities of Ag occupying specific crystallographic sites

In different Ag based compounds like Ag_2O, Ag_2NO_3 etc., it is known that Ag prefers a 2-fold coordination with stable charge state of 1+ [1,9]. In the absence of any oxidizing species during the formation of YBCO sample, Ag is also expected to remain here in 1+ charge state and will predominately attain a linear geometry with two-fold oxygen coordination. Therefore, on doping, it is unlikely to replace Ba in the YBCO structure. This oxygen coordination is similarly inconsistent with that of Y site. Considering chemical similarities, Ag substituting Cu seems most reasonable. If Ag is to partially substitute Cu in YBCO, one notes that it can do so either at Cu(2) or at Cu(1) or at both the Cu sites. However, Cu(2) has stable 2+ charge state and a fixed five-fold oxygen coordination. Ag with its 1+ charge state and two-fold oxygen coordination would not prefer to occupy Cu(2) site. The Cu(1) on the other hand can tolerate varying oxygen coordination and varying charge states including 1+. Therefore, it is expected that like other allovalent ions, Ag also preferentially substitute Cu(1).

V.3.3. Effect of Ag doping on lattice parameters

There has been a lot of controversies in the literature regarding the effect of Ag doping on the lattice parameters. While Weinberger et al. [1] have shown that Ag doping by 1.7% causes lattice expansion by about 0.8%, Cohen et al. [10] have reported that only the c parameter increases. Zhang et al. [3] have shown that both the a and c lattice parameters increase while the b parameter remains constant. Thus, there is no general agreement on the changes that Ag doping induces in the individual lattice parameters, though all

the authors mentioned above agree with the increase of unit cell volume on Ag doping. The neutron diffraction study of Taylor et al. [11], on the other hand, showed a contraction of the c-axis. Thus, to understand the variation of the lattice parameters with Ag doping in our sample, which partly agrees with Weinberger et al. [1] and Zhang et al. [3], but contradicts the result of Taylor et al. [11], we note that the lattice parameter of undoped YBCO varies with oxygen content [11]. The oxygen content determined for our samples with different Ag doping (Table V.I) shows a decrease with increasing Ag concentration. The change in lattice parameters on Ag doping in our case would therefore be a consequence of the Ag replacing Cu(1) ions and the associated oxygen loss. Comparing the lattice parameters of these samples with that of undoped YBCO samples having same oxygen deficiency, it is found that there is no appreciable changes in a, b and c parameters. Therefore, the changes that Ag doping induces on the unit cell parameters depend on the resulting oxygen deficiency. The oxygen deficiency being dependent on details of sample preparation, it is not surprising that there is no general agreement on the effect of Ag doping on unit cell parameters as reported in the literature. In addition, the fraction of Ag occupying crystallographic sites in the grains or precipitating at the grain boundaries crucially depend on sample preparation condition. The widely scattered data in the literature not being unanimous on the effect of Ag addition, clearly support this view.

Sintering at higher temperatures in oxygen atmosphere results in most of the Ag diffusing to the grain boundaries. This has been shown to result in the decrease of normal state resistivity, increase of critical current density without much affecting the superconducting transition temperature (Tc). However, sintering at relatively lower temperatures (< 900 C) under reduced atmosphere or ambient condition as the present experiment is done, results in most of Ag occupying lattice site in the grains which directly affect the superconducting and normal state properties and the lattice parameters.

V.3.4. Crystallochemical analysis of Tc variation with Ag content

Like lattice parameters, there has not emerged a general agreement on the effect of Ag doping on Tc. Some authors have reported an increase in Tc at low Ag doping regime [10,12]; others have reported that at higher concentrations of Ag, Tc decreases monotonically [4]. As has been pointed out earlier, in Ag doped systems, the associated oxygen vacancies established during sample preparation play a significant role. Our data show that both Tc and oxygen content decrease with Ag doping. As Ag is monovalent, its addition increases the hole concentration unless oxygen content is reduced. With a linear 2-fold coordination of Ag, its substitution at Cu(1) sites creates oxygen vacancies along CuO chains leaving two nearby Cu(1)s in 3-fold oxygen coordination. Our crystallochemical analysis discussed in Chapter IV shows that these 3-fold oxygen coordinated Cu(1) sites are driven to an unstable charge state and would fluctuate between two stable charge states 2+ and 1+ with consequent annihilation and creation of oxygen holes in the unit cell. The carrier concentration as well as oxygen content as shown in eqn. IV.8 would then decrease from 1 hole and 7 oxygen atoms per unit cell in undoped YBCO samples to 1-2x holes and 7-2x oxygen atoms respectively in YBCO samples doped with x Ag per unit cell.

To compare the variation of oxygen vacancy with Ag concentration as estimated from eqn. IV.9 with that observed experimentally, we choose y = 0.07 for x = 0, so that in the undoped YBCO, the starting point of both the curves coincide (Fig. V.3). The observed variation of oxygen deficiency with Ag doping has the same trend as that estimated from eqn.IV.9. The reduced oxygen deficiency at x = 0.06 may be due to excess oxygen incorporation because of the high affinity of silver for oxygen. Therefore, the factor y in eqn. IV.8, though contributes to reduced carrier concentration in undoped YBCO, gets reduced in Ag doped YBCO. The rapid decrease of oxygen content for x > 0.06 can be understood by considering the system response in the presence of excess metastable 3-fold coordinated Cu(1) centers created due to Ag doping.

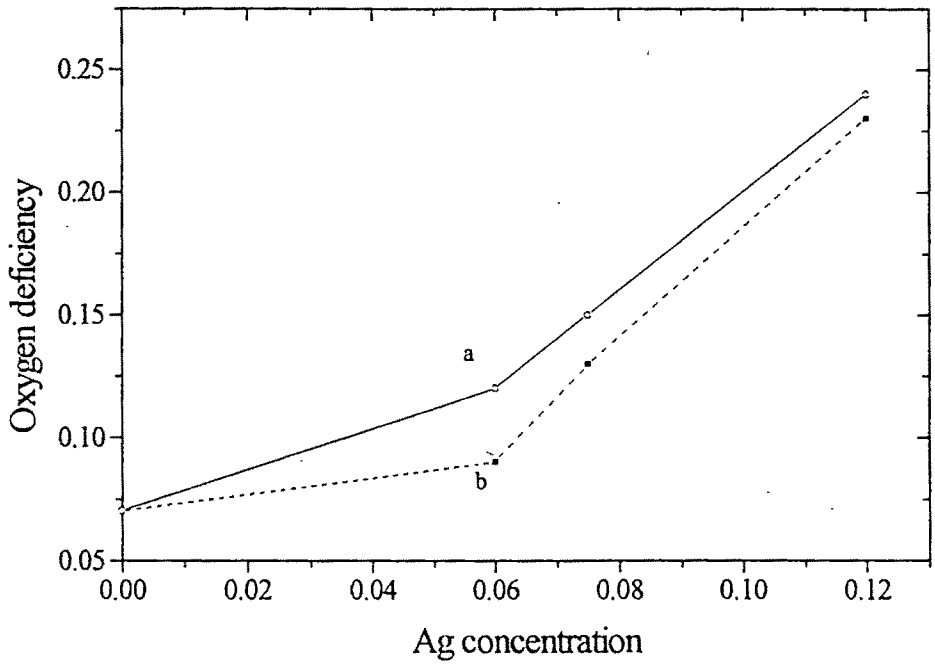

Fig. V.3. Variation of oxygen deficiency in $YBa_2Cu_{3-x}Ag_xO_{7-y}$ samples

(a) Expected value of y due to 2-fold oxygen coordination of Ag.

(b) Experimentally observed y for different Ag concentration.

As discussed earlier, with x atomic % of Ag substituting Cu(1), 2x atomic % of 3-fold oxygen coordinated Cu(1) ions emerge. These ions drive the system to a metastable state [13]. When x is beyond a critical value, the separation between these unstable centers decrease and come within a length scale where they can interact with each other. The system can come to a stabler state either by oxygen absorption, converting the 3-fold oxygen coordinated Cu(1) sites to 4-fold ones or by oxygen removal between two Ag ions occupying a single chain and converting the three fold coordinated Cu(1) ions to stabler 2-fold coordinated Cu(1) ions. Since the 2-fold oxygen coordination of Ag preclude excess oxygen intake than that estimated from eqn. IV.8, the latter process (Fig. V.4) becomes more probable, particularly when samples are prepared in ambient atmospheric conditions and not under oxygen atmosphere. Therefore, at higher Ag concentration the observed oxygen content decreases faster than that estimated from the eqn. IV.8.

In undoped YBCO the Tc vs oxygen content shows a plateau at about 90 K for oxygen deficiency $0 < y < 0.2$ (Fig. V. 5a). Fig. V.5b representing Tc vs oxygen deficiency in different Ag doped YBCO samples however shows a monotonic decrease of Tc with increasing oxygen deficiency. Therefore, for the same oxygen content, Tc is higher in undoped YBCO than in the doped one. To understand the decrease of Tc with Ag doping it is noted that Ag with its stable 2-fold oxygen coordination locks the vacancies close to its sides providing a rigidity to the CuO chains towards oxygen vacancy-mobility. This prevents spatial ordering of the arrested unstable 3-fold Cu(1)s to stabler 2-fold and 4-fold ones. In undoped YBCO, such spatial ordering, as shown in eqn. IV.4, leaves the carrier concentration unaffected. The carrier concentration however, is not the only parameter deciding the Tc value. Among other parameters, the importance of apical oxygen in the charge transfer mechanism as well as its role in pairing of the carriers due to its anharmonic vibrations leading to a strong enough coupling for high Tc has been amply emphasized [14]. Bisop et al. [15] have proposed that the dynamic displacement of the apical oxygen perpendicular to the CuO planes produce

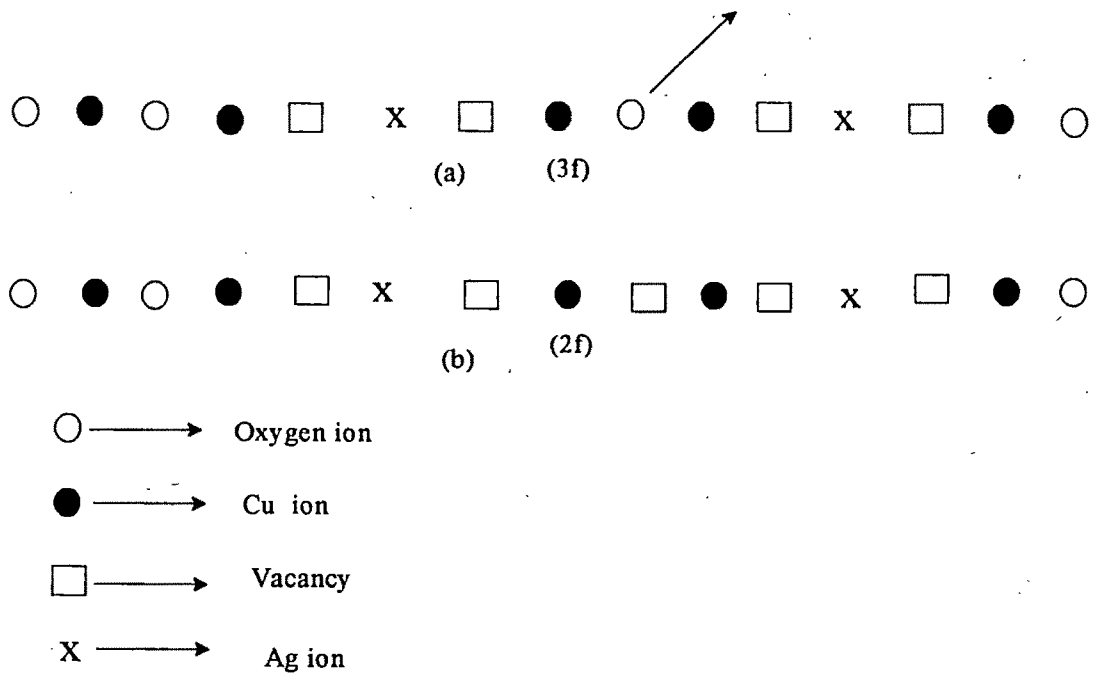

Fig. V.4. Conversion of (a) 3-fold (3f) coordinated Cu(1)s to (b) Stable 2-fold(2f) coordination in the basal plane of $YBa_2Cu_{3-x}Ag_xO_{7-y}$ through oxygen removal

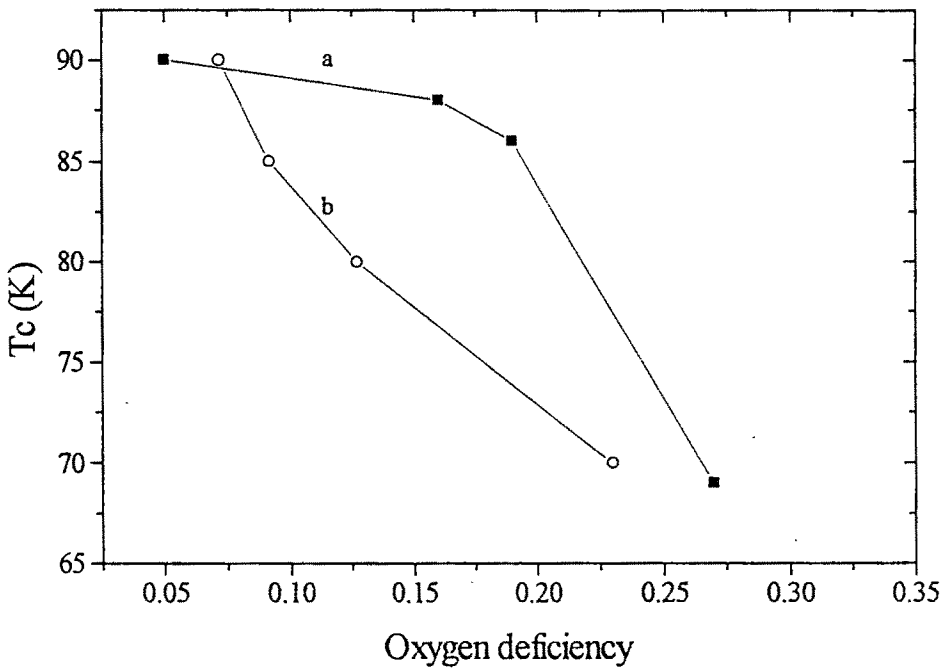

Fig.V.5. Transition temperature (Tc) dependence on oxygen deficiency in (a) $YBa_2Cu_3O_{7-y}$ and (b) $YBa_2Cu_{3-x}Ag_xO_{7-y}$ samples with x = 0.12

fluctuations of the electron-hole density and strong phonon modes along with structural instabilities in these perovskites. Further, Raman studies confirm the strong correlation of Tc with the apical oxygen vibration frequency [16]. With increasing Ag concentration, more vacancies are created in the CuO basal plane. This leads to random disorder of the BaO plane, disturbing the apical oxygen from its normal position. Such a process is expected to suppress Tc further [17].

V.3.5. Silver substitution effect on the growth of oxygen order and diffusion in quenched YBCO system

Non-equilibrium ordering has been widely studied both theoretically and experimentally in processes such as phase separation and spinoidal decomposition, order-disorder phenomena and grain growth [18]. Cuprate superconductors represents a class of 2-dimensional systems where the study of order-disorder phenomena is of considerable interest from both theoretical and experimental point of view. In YBCO system both overall oxygen content and ordering of oxygen in the basal plane of the unit cell play an important role in deciding superconducting and normal state properties. The superconducting transition temperature, Tc in particular varies linearly with the relative occupancy of oxygen in the chains along the b-axis as compared to that in a-axis. The ordering has been shown to crucially depend on the thermal history of the sample and on initial oxygen configuration [19]. At lower oxygen content, though the sample exhibit an overall tetragonal structure, the local ordering in the form of chain fragments are crucial for Tc. Depending upon the oxygen stoichiometry, the two distinct phases, ortho-I and ortho-II develop with Tc = 90 K and 60 K respectively. Dynamics of ordering in both the phases have been shown to be characterized by a non-conserved order parameter with Lifshitz-Allen-Kahn growth mechanism. At the transition region from 90 K ortho-I phase to the 60 K ortho-II phase, many short range ordered full-empty chain arrays have been observed by electron

microscopy which revealed superlattice formation in two or three dimensions. For very low oxygen concentration, room temperature (RT) annealing of thermally quenched samples have been shown to result in Tc increase and higher orthorhombicity due to layered domains of ordered atoms. Superconductivity has been shown to depend crucially on the size of these domains. Most of the studies have been confined to single crystals providing length scale much larger than the chain fragments. Dynamics of ordering in the grains of smaller dimensions with larger surface to volume ratio is not clear. The effect of grain boundary, particularly on the growth of order is still illusive. In this section we study the dynamics of oxygen ordering in grains and probe the effect of grain boundaries in YBCO and Ag (0.12 atoms per unit cell) doped YBCO, where the initial disordered state was induced by quenching from high temperature.

Fig. V.6 shows the effect of quenching and RT annealing on the temperature dependence of A.C magnetic susceptibility of undoped YBCO sample. On quenching from 500 K, the sample showed a superconducting transition with a Tc_{on} of 75 K. Annealing of this quenched sample at RT for two hours, however caused a decrease Tc_{on} to 67 K instead of the expected increase. This value of Tc_{on} did not change further on prolonged annealing. The Ag doped sample, on the other hand, showed the opposite behaviour. The quenched sample had a Tc_{on} of 77 K which increased to 88 K on annealing at RT for 2 hrs (Fig. V.7) and remained at this value on further annealing.

It has been established by many [20,21] that Tc in YBCO systems depend on the ordering of oxygen in the basal plane. Veal et al. [22] and Shaked et al. [21] have shown that under annealing of quenched YBCO samples at RT, ordering in the basal plane occurs with consequent rise in orthorhombicity and Tc. Our result for undoped granular YBCO sample however show a different behaviour. The quenched (from 500 C to RT) sample showed a higher Tc_{on} (75 K) than the Tc_{on} (67 K) of the annealed sample. To understand this unusual behaviour we note that the samples used

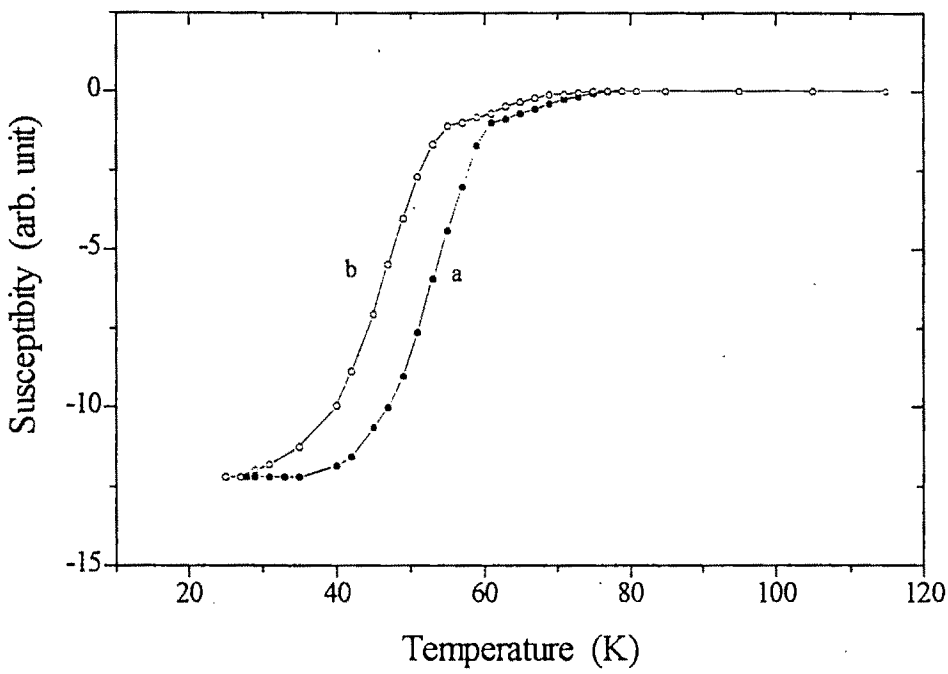

Fig.V.6. AC magnetic susceptibility variation with temperature in $YBa_2Cu_3O_{7-y}$ samples (a) quenched from 500 C (b) quenched from 500 C and annealed for 2hrs.

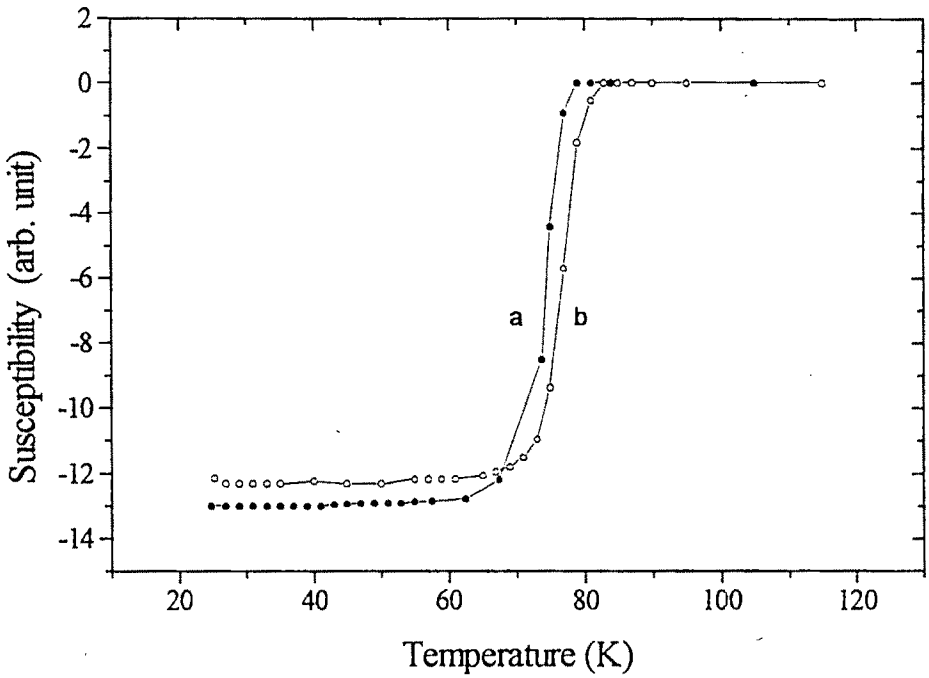

Fig.V.7. AC magnetic susceptibility variation with temperature in $YBa_2Cu_{3-x}Ag_xO_{7-y}$ samples with x = 0.12 (a) quenched from 500 C (b) quenched from 500 C and annealed for 2hrs.

by [21,22] were single crystals whereas polycrystalline pellets where grain boundaries play significant role were used in our case.

Sintering at 500 C introduces two distinct changes in the samples: i. the loss of oxygen from the grain boundaries due to desorption and ii. disorder of oxygen in the basal plane. Oxygen loss at the grain boundaries has been confirmed by TG/DTA studies which show that increasing temperature increases oxygen absorption upto 300 C and further rise in temperature leads to desorption of oxygen [23]. Such a process leaves the grain boundaries oxygen deficient with the interior of the grains still having higher oxygen content. This introduces oxygen concentration gradient from the interior to the boundary of each individual grain. This gradient acting like a driving force would equalize the oxygen concentration throughout the grain. The second process involves disordering of oxygen on quenching and would lead to a more ordered state on annealing at RT.

The effect of the two processes; equalization of oxygen content due to oxygen diffusion from interior of the grains towards the boundary and ordering of the disordered oxygens on the Tc is expected to be opposite. While the interior of the grains with higher oxygen content than that at the grain boundaries would result into a higher Tc in quenched samples, the oxygen disorder induced due to quenching would lead to a lower Tc. On annealing at RT, the Tc would decrease due to the first process due to less overall oxygen in the grains and increase due to the second process due to more ordered oxygen chains. The time scales involved in the two processes however is very different. Because of the next nearest neighbour interaction involved in the oxygen ordering process [24], this process is much faster than the oxygen diffusion process. The ordering process also becomes still faster at higher oxygen content [21]. Thus, during quenching itself, oxygen ordering takes place leading to high Tc as observed. Annealing at RT however leads to oxygen diffusion from the interior of the grains towards the grain boundaries reducing the overall oxygen content and suppressing the Tc.

In Ag doped sample (Fig. V.7), RT annealing after quenching leads to increase of Tc unlike that in case of undoped YBCO sample (Fig. V.6). As discussed earlier, Ag preferentially occupies Cu(1) sites in the CuO chain. Unlike Cu, Ag has a fixed 2-fold oxygen coordination and leaves two vacancies near the Ag ions in the chains. Diffusion of oxygen from the interior of the grains which ordinarily would fill the vacant sites on the grain boundaries in YBCO, is prevented from doing so in Ag doped sample. This effect of Ag confines the oxygen in the interior of the grains and does not allow them to diffuse to the grain boundaries leaving the Tc unaffected. The observed rise in Tc in this case is because of the oxygen ordering.

The oxygen content of undoped YBCO showed stronger dependence on quenching temperature (Fig. V.8a) and the values obtained agree with the reported data [25]. The Ag doped YBCO however showed a much weaker dependence of oxygen content on quenching temperature (Fig. V.8b). While undoped YBCO had lower oxygen content than Ag-doped YBCO when quenched from 700 and 900 C, reverse effect occurred for samples quenched from 500 C and 300 C.

Oxygen stoichiometry in YBCO is known to be influenced by oxygen in/out diffusion. The oxygen diffusion process is strongly dependent on the sintering temperature. The total oxygen uptake by the YBCO lattice shows a maximum around 300 C and sharply falls beyond the orthorhombic-tetragonal phase transition around 600 C [23]. In the tetragonal phase, the oxygen out diffusion dominates [26] resulting in a very low oxygen content for samples quenched from 700 C and 900 C. In Ag doped samples however, Ag occupying Cu(1) sites locks the oxygen vacancies around it along the chains and blocks the out-diffusion process. This results in higher oxygen content for samples quenched from 700 C and 900 C. Since in-diffusion dominates for samples quenched in the orthorhombic states i.e. for 300 C and 500 C, the undoped system showed higher oxygen content. Under the similar situation, Ag doped samples showed lower oxygen content due to Ag locking the vacancies in the chains and blocking the diffusion process.

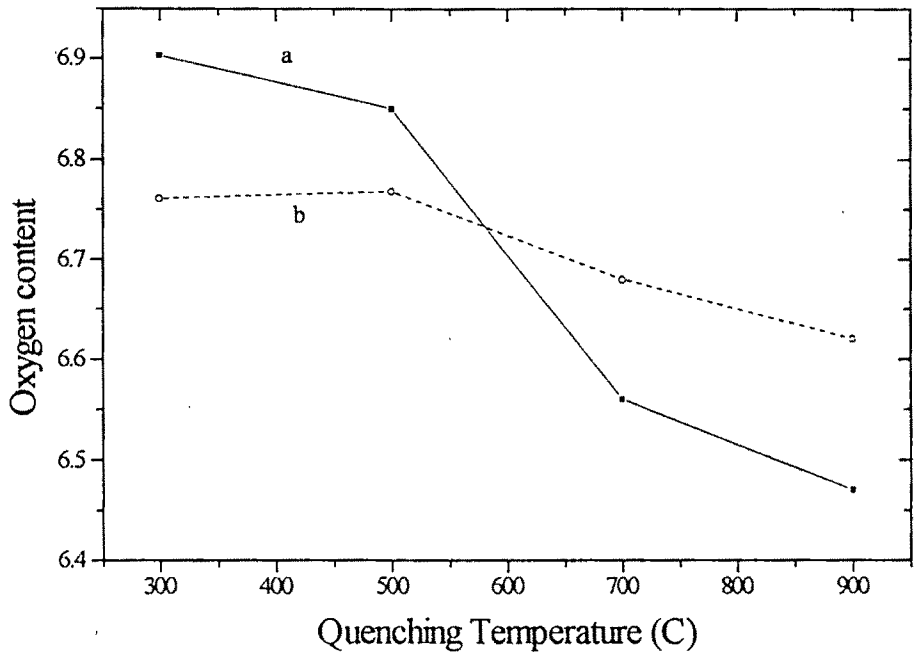

Fig.V.8. Variation of oxygen content with quenching temperature in (a) $YBa_2Cu_3O_{7-y}$.sample (b) $YBa_2Cu_{3-x}Ag_xO_{7-y}$ sample with x = 0.12

V.4. Conclusion

The present study shows that with $YBa_2Cu_{3-x}Ag_xO_{7-y}$ samples prepared at relatively lower temperature and ambient atmospheric condition, precipitation of Ag to the grain boundaries can be prevented. The effect of Ag doping on the lattice parameters and Tc is explained on the basis of its effect on the oxygen content in YBCO due to its fixed 2-fold oxygen coordination. The fixed two fold oxygen coordination of Ag also provides rigidity to the CuO chains and prevents oxygen in/out diffusion as evidenced from quenching experiments.

References

1. B.R. Weinberger, L. Lynds, D.M. Potrepka, D.B. Snow, C.T. Burila, H.E. Eaton Jr.,R.Cipolli, Z. Tan, and J.I. Budnick, Physica C **161** (1989) 91.
2. L. Dominic, S. Kamel, Japanese Journal of Applied Phys. **29** (1990) L 2017.
3. C. Zhang, A. Kulpa, A.C.D. Chaklader, Physica C **252** (1995) 67.
4. A.K. Gangopadhyay, and T.O. Mason, Physica C **178** (1991) 64.
5. J. Joo, J.P. Singh, R.B. Poeppel, A.K. Gangopadhyay, and T.O. Mason, J. Appl. Phys. **71** (1992) 2351.
6. C.N.V. Huong, E. Crampin, J.Y. Laval, A. Dubon, Supercond. Sci. Technol. **10** (1997) 85.
7. T.S. Orlova, J.Y. Laval, A. Dubon, C.N.V. Huong,, B.I. Smirnov, P.Yu. Stepanov, Supercond. Sci.Technol. **11** (1998) 467.
8. K. Yamamo, H. Mazaki, H. Yasuoka, S Katsuyama, K. Kosuge, Physical Rev. B **46** (1992) 1122.
9. J.V. Anderson, Physica C **214** (1993) 143.
10. D. Cohen, C.C. Sorrell, S.X. Dou and M. Apperley, J. Am. Ceram. Soc. **74** (1991) 1541.

11. C.R. Taylor, and C. Greaves, Physica C **235-240** (1994) 853.
12. M.N. Khan, S.Al Dalla and A. Menon, International Journal of Modern Physics B **4** (1990) 1993.
13. H.P. Mohapatra, D. Behera, B. Dash, N.C. Mishra, and K. Patnaik, Physica C **185-189** (1991) 739.
14. K.A. Muller, Z. Phys. B **80** (1990) 193.
15. A.R. Bishop, R.L. Martin, K.A. Muller, Z. Phys. B **76** (1989) 17.
16. K. Matsuishi, Y.K. Tao, H.S. Feng, P.H. Horr and C.W. Chu, Physica C **185-189** (1991) 827.
17. Y. Kazuhiko, O. Yoshoshi, Y. Takaaki, D. Mikihiko and I. Fuminori, Physica C **185-189** (1991) 1237.
18. T. Christen, Euro Phys. Lett. **31** (1995) 181.
19. R.J. Cava, A.W. Hewat, E.A. Hewat, M. Marezio, K.M. Rabe, J.J. Krajewski, M.F. Peck Jr. and I.W. Rupp Jr., Physica C **165** (1990) 419.
20. J.D. Jorgensen. S. Pei, P. Lightfoot, H. Shi, A.P. Paulikas and B.W. Veal, Physica C **167** (1990) 571.
21. H. Shaked, J.D. Jorgensen B.A. Hunter, R.L. Hitterman, A.P. Paulikas and B.W. Veal, Phys. Rev. B **51** (1995) 547.
22. B.W. Veal, H. You, A.P. Paulikas, H. Shi and J.W. Downey, Phys. Rev. B **42** (1990) 4770.
23. J.R. Lagraff, P.D. Pines, Phys. Rev. B **43** (1991) 441.
24. L.T. Wille, Phys. Rev. B **40** (1989) 6931.
25. C. Namgung, J.T.S. Irvine and A.R. West, Physica C **168** (1990) 346.
26. J.R. Lagraff and D.A. Pyne Physica C **212** (1993) 470.